

Classification of gastric pit patterns by confocal endomicroscopy

Jian-Na Zhang, MD, Yan-Qing Li, MD, PhD, You-An Zhao, MD, Tao Yu, MD, Jian-Ping Zhang, MD, Yu-Ting Guo, MD, Hong Liu, MD

Jinan, China

Background: Confocal endomicroscopy is a newly developed endoscopic imaging technology that produces 1000-fold magnification cross-sectional images of the GI surface and subsurface tissue during routine endoscopy. The gastric pit patterns identified by confocal endomicroscopy and correlation with histopathologic examination have not yet been established.

Objective: Our purpose was to explore the appearance of various kinds of gastric pits and clarify the relationship between gastric pit patterns and the histopathologic findings.

Design: Descriptive study.

Setting: Qilu Hospital, Shandong University, Jinan, China.

Patients: A total of 132 consecutive patients underwent confocal endomicroscopy after 7 healthy volunteers had been examined in vivo and 10 samples resected from 10 patients with gastric cancer had been examined ex vivo by use of confocal endomicroscopy. The confocal images obtained from the 132 patients were compared with the histopathologic findings of the biopsy specimens from the corresponding confocal imaging sites in a prospective and blinded fashion.

Main Outcome Measurements: The relationship between the pit patterns and the histopathologic findings.

Results: Gastric pit patterns were classified into 7 types. Normal mucosa with fundic glands mainly showed type A (round pits), and corporal mucosa with histologic gastritis showed type B (noncontinuous short rod-like); normal mucosa with pyloric glands mainly showed type C (continuous short rod-like), and antral mucosa with histologic gastritis showed type D (elongated and tortuous branch-like). Goblet cells were easily distinguished by confocal endomicroscopy in intestinal metaplasia mucosa, which showed type F. The sensitivity and specificity of the type E pattern for predicting gastric atrophy were 83.6% and 99.6%, respectively. Corresponding values of the type G pattern for predicting gastric cancer were 90.0% and 99.4%.

Limitations: No data on interobserver and intraobserver variability.

Conclusions: The patterns of gastric pits identified by confocal endomicroscopy correlate well with the histopathologic findings. Confocal endomicroscopy may prove useful in predicting histopathologic diagnoses during routine endoscopic procedures. (*Gastrointest Endosc* 2008;67:843-53.)

The main purpose of GI endoscopy is to detect lesions and to determine the qualitative diagnoses of the lesions on the basis of benign and malignant features; however, sometimes the differentiation of malignant from benign lesions is not easy. The ultimate diagnosis has to be confirmed by taking endoscopic biopsy specimens. Fortunately, the

newly developed technique of confocal endomicroscopy provides a convenient method of differentiating malignant from benign lesions because confocal endomicroscopy has the ability to observe the surface and subsurface architecture of the GI tract at the cellular level during standard white-light endoscopy.^{1,2}

However, the cross-sectional virtual histologic images obtained in vivo by confocal endomicroscopy¹ are obviously different from those found by conventional histopathologic examination. It is very important for the endoscopists performing confocal endomicroscopy to master the features of confocal images of all kinds of lesions on which the diagnosis is based. The gastric pits, openings of glands in

Abbreviations: NPV, negative predictive value; PPV, positive predictive value.

Copyright © 2008 by the American Society for Gastrointestinal Endoscopy
0016-5107/\$32.00
doi:10.1016/j.gie.2008.01.036

the stomach, are the basic units of the microstructures on the surface of gastric mucosa. The gastric pit pattern shows complicated changes in inflammatory and neoplastic (pre-malignant and malignant) lesions under magnifying endoscopy.³⁻¹⁰ Similarly, the changes can be observed by confocal endomicroscopy that has the ability to produce 1000-fold magnification images. Several investigators have reported the usefulness of confocal endomicroscopy in colorectal cancer,¹¹ collagenous colitis,¹² and gastric cancer.^{13,14} But there has not been any report on the characterization and classification of gastric pit patterns; therefore, an attempt was made in the current study to determine the classification of gastric pit patterns by confocal endomicroscopy and the relationship between the patterns of gastric pits and relevant histopathologic findings.

PATIENTS AND METHODS

Confocal endomicroscope

Confocal endomicroscopy is the integration of a miniaturized laser scanning confocal microscope (Optiscan, Notting Hill, Victoria, Australia) into the distal tip of a conventional endoscope (EC-3870K, Pentax, Tokyo, Japan). This technology allows conventional white-light endoscopy and confocal microscopy to be done simultaneously. Confocal microscopy is well suited to the visualization of microscopic structures in intact tissues and generates a sequence of high-resolution fluorescent images from successive focal planes within the specimen. During confocal endomicroscopy, actuation of imaging plane depth was controlled by using 2 handpiece buttons. Confocal images were collected at a scan rate of 1.6 frames per second (1024×512 pixels) or 0.8 frames per second (1024×1024 pixels). The optical slice thickness was 7 μm , and the lateral resolution was 0.7 μm . The range of z-axis was 0 to 250 μm below the contact surface. The field of view was $475 \times 475 \mu\text{m}$. The confocal images and endoscopic images could be produced simultaneously.

Patients

During the early period of the study, a total of 10 patients (7 men, 3 women; age range 42-75 years, median age 59.5 years) with gastric cancer who were scheduled to have operations and 7 healthy volunteers (4 men, 3 women; age range 30-63 years, median age 37 years) were recruited. Before surgery, all the patients were asked whether samples resected could be used for examination *ex vivo* with confocal endomicroscopy, and written informed consent was obtained. Written informed consent was also obtained from all 7 healthy volunteers.

From June 2006 to November 2006, 132 consecutive patients with GI symptoms who were scheduled to have endoscopic examinations were enrolled in the subsequent study at Qilu Hospital, Shandong University, China. Exclusion criteria were liver cirrhosis, impaired renal function,

Capsule Summary

What is already known on this topic

- Confocal endomicroscopy provides 1000-fold magnification and cross-sectional, virtual histologic images, but its accuracy for differentiating gastric pit patterns in inflammatory and neoplastic lesions has not been established.

What this study adds to our knowledge

- In a blinded prospective study of gastric pit patterns identified by confocal endomicroscopy in 132 patients, the diagnostic accuracy for atrophy and gastric cancer was 97.5% and 97.1%, respectively.

acute GI bleeding, coagulopathy, esophageal varices, jaundice, age < 18 years old, pregnancy or breast-feeding, inability to provide informed consent, and known allergy to fluorescein. Of the 132 patients, 47 patients had abdominal pain, 38 patients had epigastric discomfort, 34 patients had acid regurgitation, 32 patients had abdominal distention, 29 patients had nausea or accompanying vomiting, and 27 patients had belch (each patient had one or more predominant symptoms). Written informed consent was obtained from all participating patients before the procedure. This protocol was approved by the ethics committee of our hospital and conducted according to the Helsinki Declaration.

Endoscopic procedure

The samples resected from 10 patients with gastric cancer were examined *ex vivo* by confocal endomicroscopy. The acriflavine (0.05%) was applied topically to the sample, and after the mucosa had been stained for 1 to 3 minutes the excess contrast was washed off with normal saline solution. Afterward, the samples were examined by confocal endomicroscopy. The 7 healthy volunteers and 132 patients underwent confocal endomicroscopy. Preparation of patients for the confocal examination was the same as that for standard upper endoscopy. The confocal endoscopy was conducted by 3 senior endoscopists (L. Y, Z. Y, and Y. T). Routine endoscopy was first performed by using the nonconfocal function; 500 mg of fluorescein sodium was administered intravenously as a contrast agent after the operator had decided to perform confocal endomicroscopy. In the process of confocal endomicroscopy, the target area for imaging was placed at the lower left corner of the endoscopic view and confocal lens was placed in contact with the mucosa by use of the blue laser guide; gentle pressure was exerted to maintain mucosal contact and apply suction during the active phase of imaging. Confocal observation was possible from about 10 seconds after the intravenous injection of fluorescein to 10 to 15 minutes afterward. The

The classification of gastric pit patterns by confocal endomicroscopy

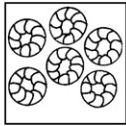
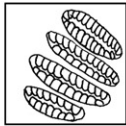
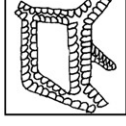
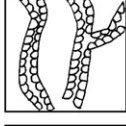
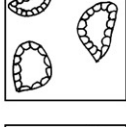
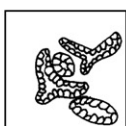
Category	The appearance of pit patterns by confocal endomicroscopy	Distribution area	Diagram
Type A	Round pits with round opening	Normal mucosa with fundic gland	
Type B	Non-continuous short rod-like pits with short thread-like opening	Corporal mucosa with chronic inflammation	
Type C	Continuous short rod-like pits with slit-like opening	Normal mucosa with pyloric gland	
Type D	Elongated and tortuous branch-like pits	Antral mucosa with chronic inflammation	
Type E	The number of pits decreasing and pits prominently dilating	Chronic atrophy gastritis	
Type F	Villus-like appearance, interstitium in the centre and goblet cells appearing	Intestinal metaplastic mucosa	
Type G			
Type G ₁	Normal pits disappearing, with the appearance of diffusely atypical cells	Signet-ring cell carcinoma and poorly differentiated tubular adenocarcinoma	
Type G ₂	Normal pits disappearing, with the appearance of atypical glands	Differentiated tubular adenocarcinoma	

Figure 1. The classification of gastric pit patterns by confocal endomicroscopy.

standardized location (the greater and lesser curvature of the antrum, both within 2 to 3 cm from the pylorus, the middle portion of the greater curvature of the corpus, and the lesser curvature of the corpus about 4 cm proximal to the angulus) and every macroscopic lesion, such as erosion, ulcer, the change of color, and abnormal fold, were examined with the confocal laser imaging system. All images were stored as digital files available for reanalysis after the procedure.

Design of data analysis

During the early period of the study, the confocal images obtained from 10 resected specimens and 7 healthy volunteers and the histopathologic findings were reviewed by an expert pathologist (Z. J.) and 2 expert endoscopists (Z. J. and L. Y.) familiar with confocal endomicroscopy in an unblinded manner. Insight gained from the exploratory meeting and from previously published classification when using magnification endoscopy³⁻¹⁰ was used to develop the

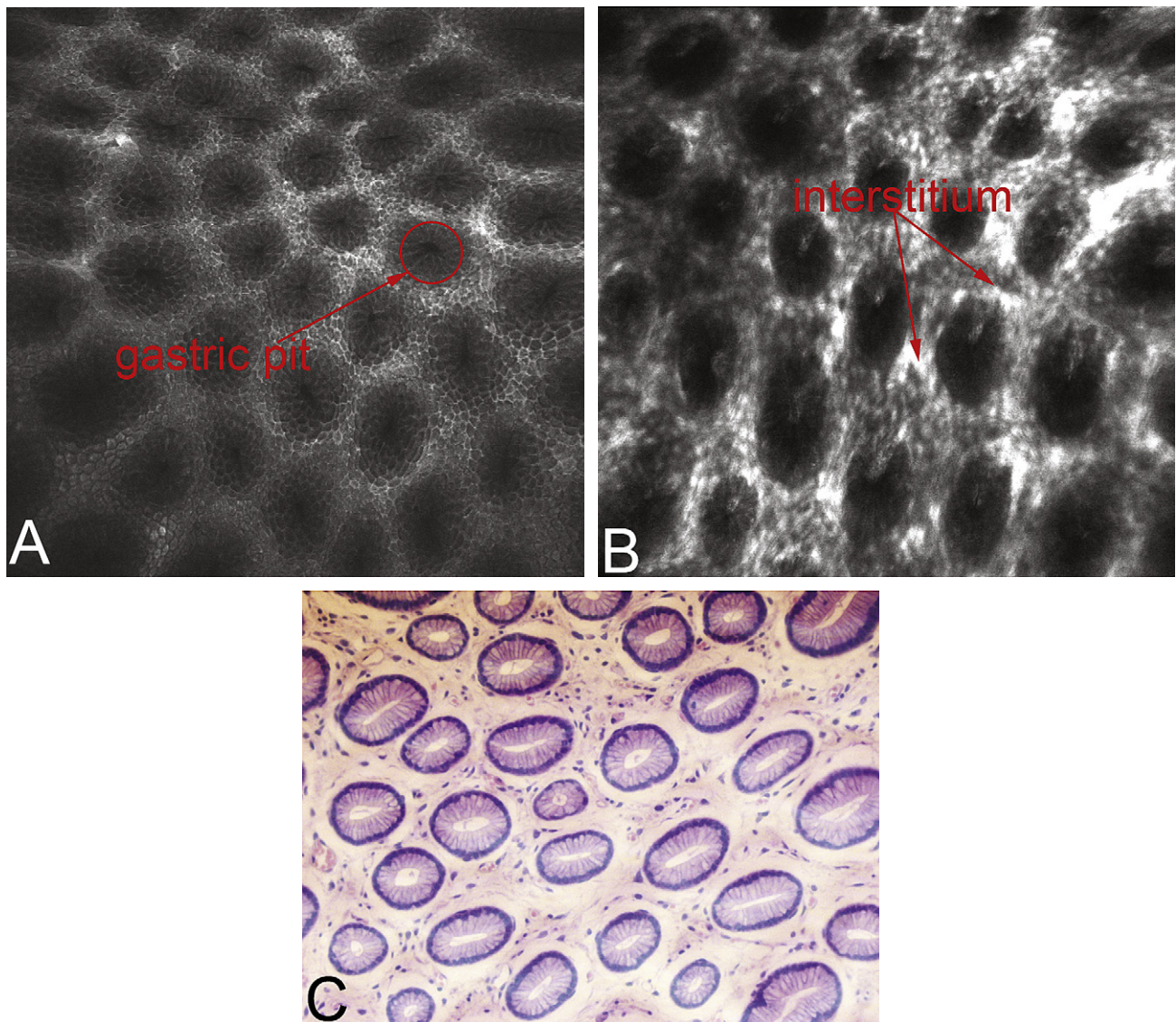


Figure 2. The confocal and corresponding histologic images of normal mucosa with fundic glands in the stomach. Round gastric pits of approximately uniform size and shape (type A). **A**, The surface gastric pits. The gastric pit is composed of columnar cells and round opening. **B**, The subsurface (below superficial epithelial cells) gastric pits. Interstitium between gastric pits can be seen. **C**, The corresponding cross-sectional histologic features of type A (H&E, orig. mag. $\times 400$).

classification of gastric pit patterns by confocal endomicroscopy. The classification was then prospectively applied to a “validation set” (the 132 patients). The examined results of 7 healthy volunteers and 10 resected specimens used for the exploratory evaluation were excluded from the subsequent analysis.

Comparison of confocal images with histopathologic examination

Biopsy specimens were obtained with standard biopsy forceps from the sites where the objective lens of the confocal microscope made contact. The specimens were fixed with 10% formalin and embedded in paraffin, and sections

were stained with hematoxylin and eosin for routine histopathologic examination. According to the Updated Sydney System, chronic inflammation, polymorphonuclear neutrophil activity, and glandular atrophy were graded as normal, mild, moderate, and severe.¹⁵ The histopathologic diagnostic criteria of gastric cancer were based on the World Health Organization classification system.¹⁶ All biopsy sections were examined independently by 1 experienced GI pathologist (Z. J.) blinded to the confocal endoscopic findings. To compare the pit patterns prospectively with histopathologic findings before histopathologic results were available, the 2 investigators (Z. J. and L. Y.) who had participated in the conceptualization of the confocal pit patterns analyzed the recorded confocal images and recorded the pit

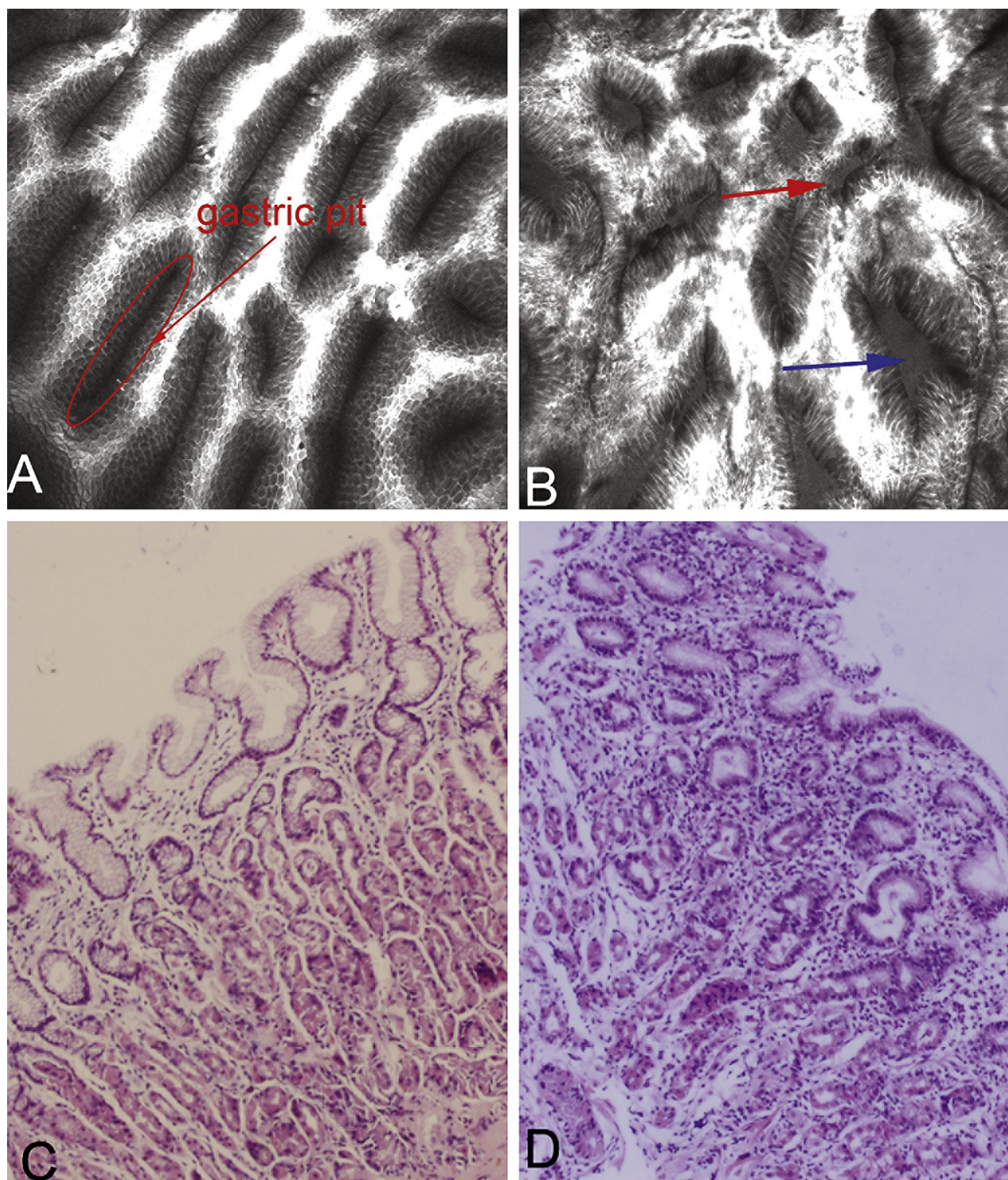


Figure 3. The confocal and corresponding conventional histopathologic images of the pattern of type B and B'. **A**, Noncontinuous short rod-like pits (type B), appearing in the corporal mucosa with chronic inflammation. **B**, The pattern of type B', the dilated lumen of gastric pit (*blue arrow*), and the defect of epithelial cells (*red arrow*) can be seen in the corporal mucosa with moderate to severe neutrophil activity. **C**, The histopathologic findings of type B. Moderate inflammation in the corporal mucosa is identified according to the updated Sydney System. **D**, The histopathologic findings of type B'. This can be diagnosed as severe inflammation and moderate neutrophil activity in the corpus mucosa according to the updated Sydney System (H&E, orig. mag. $\times 200$).

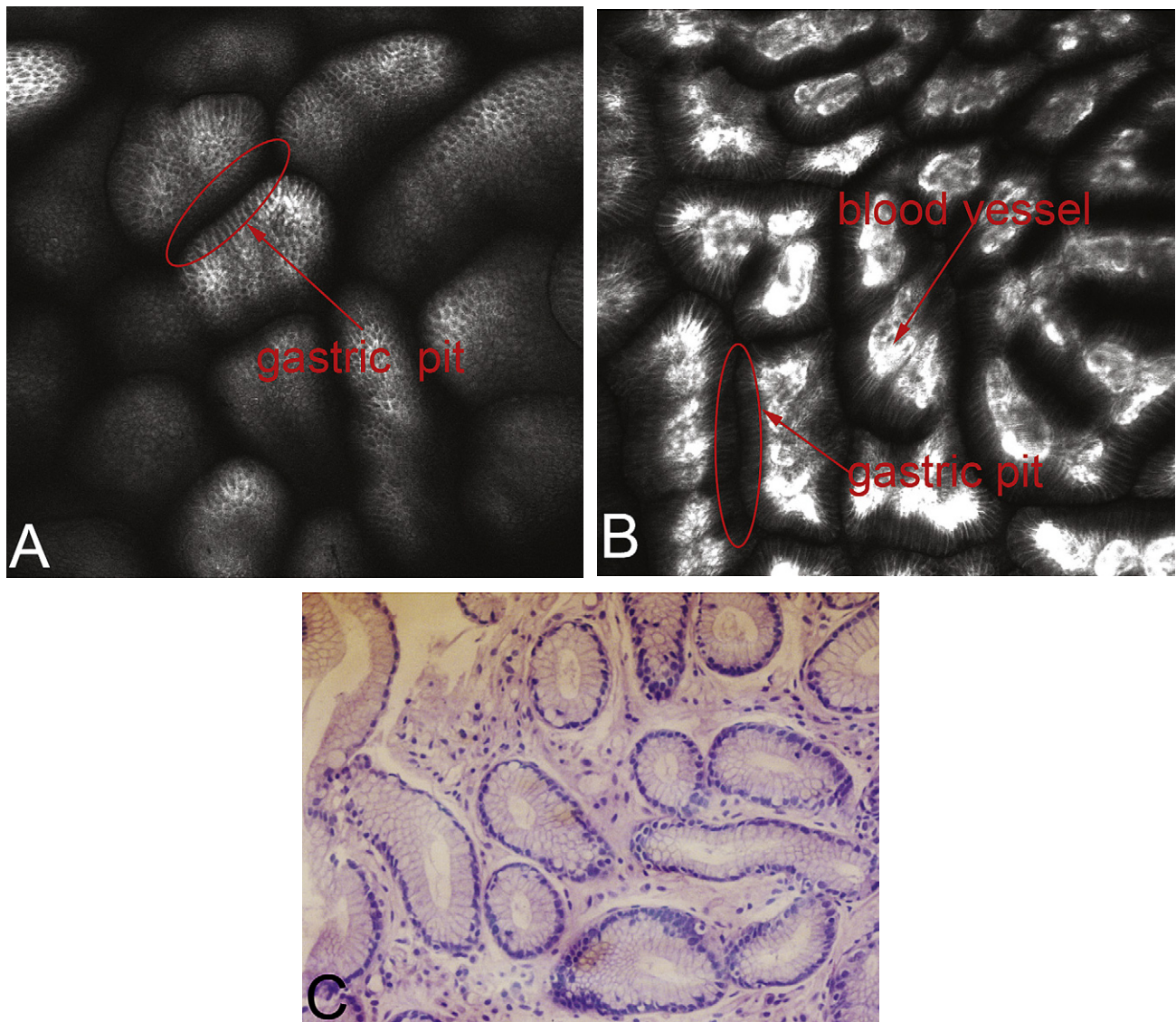


Figure 4. The confocal and corresponding histologic images of normal mucosa with pylori glands in the stomach. Continuous short rod-like pits with approximately uniform length (type C). **A**, The surface gastric pits and **(B)** the subsurface gastric pits. The width of interstitium between pits and that of pits themselves is about the same, and the coil-shaped blood vessels can be seen. **C**, The corresponding cross-sectional histologic features of type B. (H&E, orig. mag. $\times 400$.)

patterns and the predictions for histopathologic findings on preprinted forms. If there was a difference of opinion, agreement was attained by discussion.

Statistical analysis

All data were entered and stored in a computerized database designed with Microsoft Excel 2000. The statistical analysis was performed by using the statistical software package SPSS 13.0 (SPSS, Chicago, Ill). The inflammatory degree between the 2 groups was compared by the Mann-Whitney *U* test. *P* values less than .05 were considered significant. The sensitivity, specificity, positive predictive value (PPV), negative predictive values (NPV), and accuracy of different types of confocal pit patterns for the prediction

of atrophy, moderate and severe neutrophil activity, and gastric cancer were calculated. The histologic findings were used as the reference standard of diagnosis.

RESULTS

Clinical features of the patients

The sample of 132 patients included 113 patients with chronic gastritis, 8 patients with gastric ulcer, and 11 patients with gastric cancer (8 patients with signet-ring cell carcinoma or poorly differentiated tubular adenocarcinoma and 3 patients with differentiated tubular adenocarcinoma). Because it was not easy to make the objective lens of the confocal microscope have close contact with

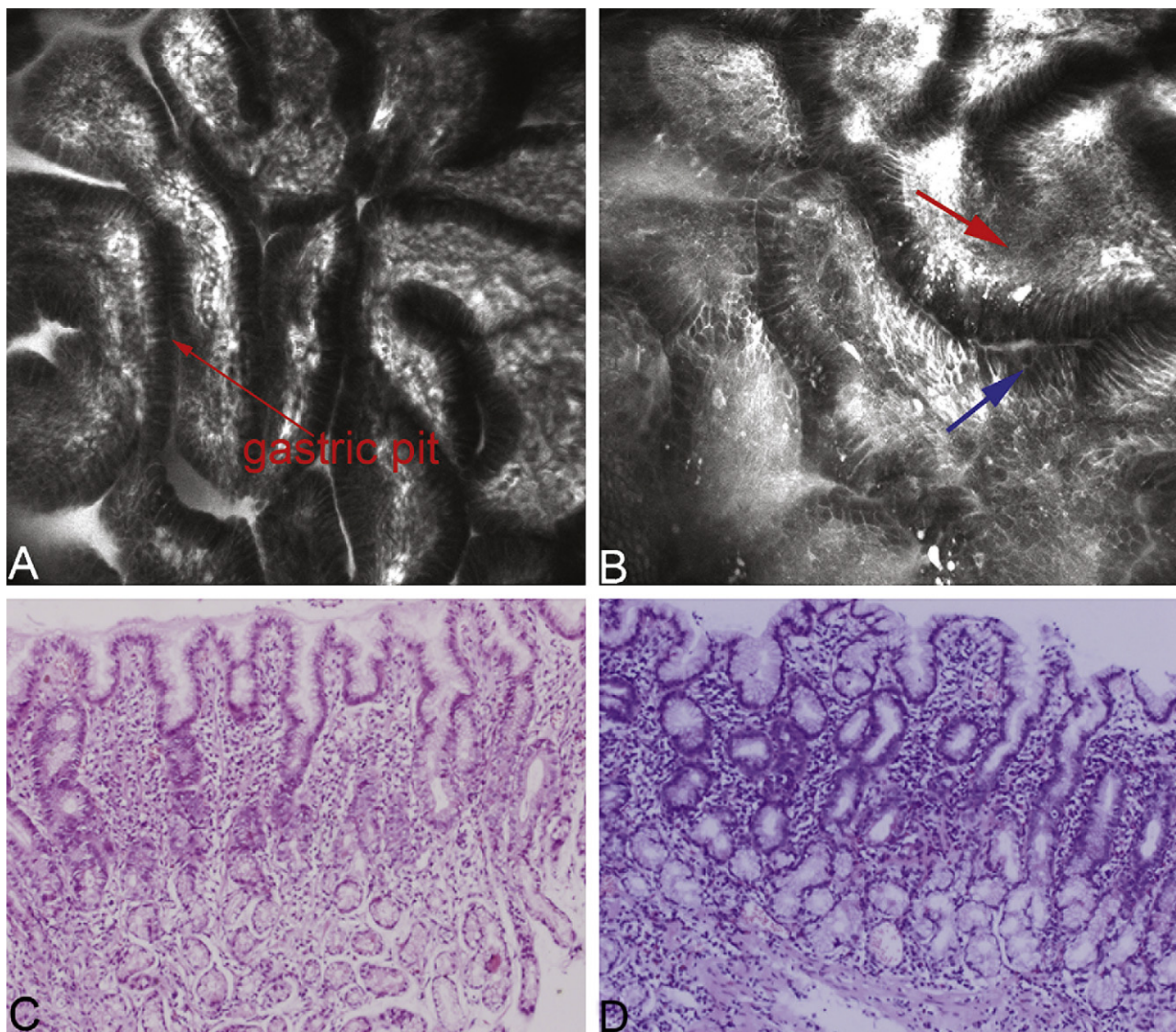


Figure 5. The confocal and corresponding conventional histopathologic images of the pattern of type D and D'. **A**, The pattern of type D, elongated and tortuous branch-like pits, appearing in the antral mucosa with chronic inflammation. **B**, The pattern of type D'. The interstitium widening between 2 pits (*red arrow*) and the swelling epithelial cells (*blue arrow*) can be seen in the antral mucosa with moderate to severe neutrophil activity. **C**, The histopathologic findings of type D. The moderate inflammation in the antral mucosa is identified according to the updated Sydney System. **D**, The histopathologic findings of type D'. This can be diagnosed as severe inflammation and moderate neutrophil activity in the antral mucosa according to the updated Sydney system (H&E, orig. mag. $\times 200$).

elevated-type lesions, such as polyps and gastric adenoma, these lesions were excluded from the study. Confocal images—10,564 from 556 different locations—were obtained and compared with the histopathologic findings from corresponding biopsy specimens. Of 556 sites where confocal images were obtained, 35 were excluded because of poor image quality, leaving a total of 521 biopsy-correlated images for analysis. As a result, 10,123 of the original 10,564 images were actually analyzed.

Pit patterns and histopathologic findings

Confocal endomicroscopy was able to visualize precisely the structure of pits. The gastric pit patterns were classified

into 7 types. Figure 1 shows the diagram of the 7 pit patterns, and Figures 2 through 8 represent the confocal images of the 7 pit patterns. In addition, in type B, there was a subtype type B', and the dilated lumens of gastric pits or the defect of topical epithelial cells of pits could be seen in it, indicating corporal mucosa with moderate to severe neutrophil activity (Fig. 3B); in type D, there was a subtype, type D', and the widened interstitium between 2 pits or the defect of topical epithelial cells of pits could be seen in it, indicating antral mucosa with moderate to severe neutrophil activity (Fig. 5B).

Among the 109 sites classified as type A and 93 sites classified as type B, the histopathologic results for grading

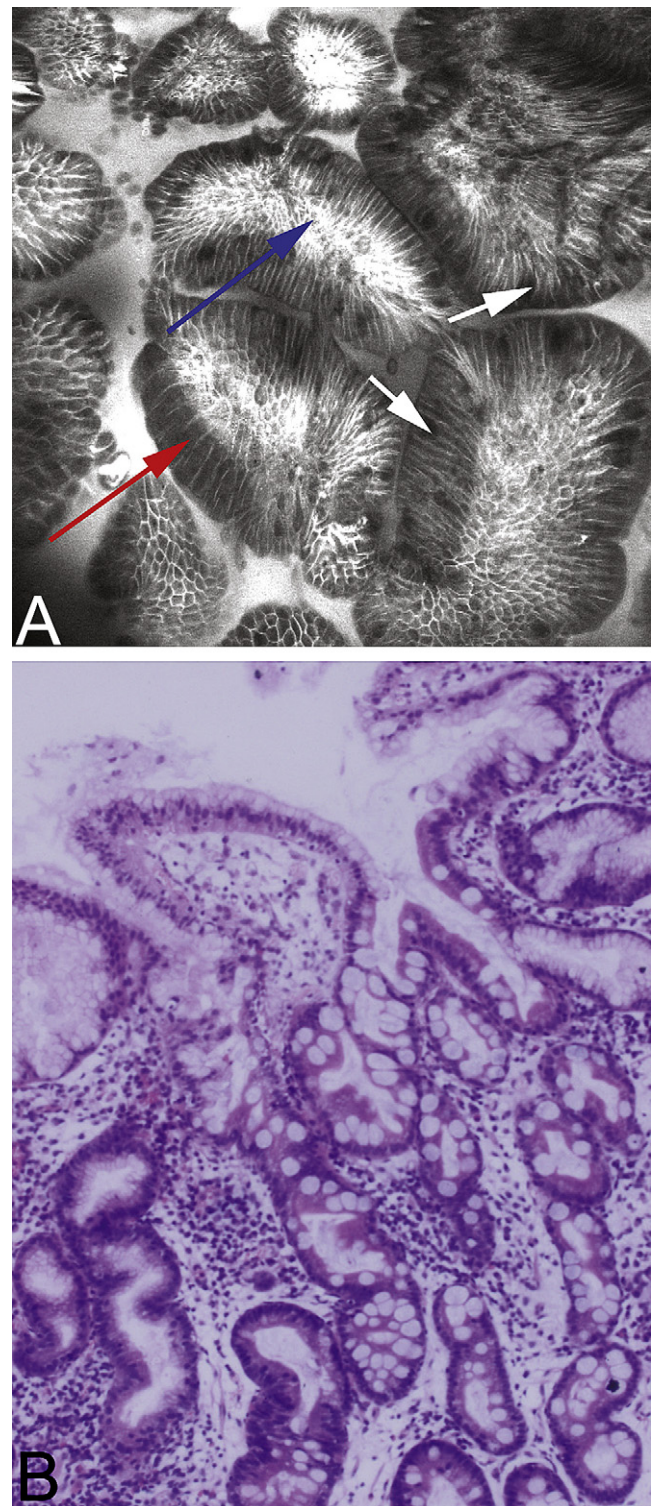
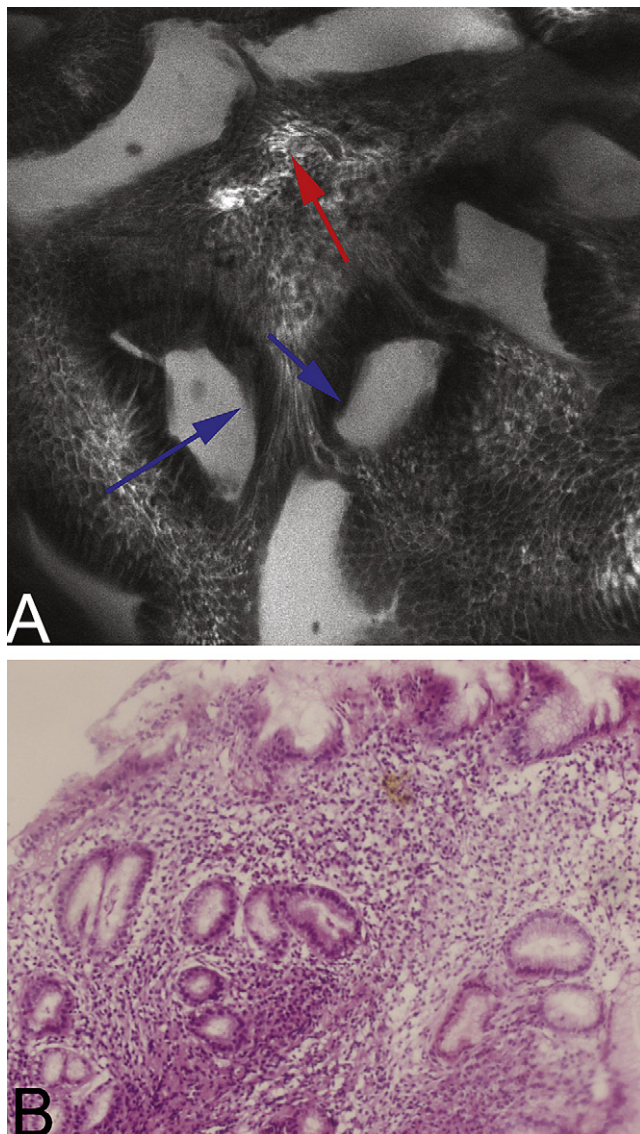


Figure 6. The confocal image of the pattern of type E and the histopathologic features of type E. **A**, The number of pits decreasing and the lumens of pits prominently dilating (*blue arrow*). The blood vessels (*red arrow*) can be seen at the surface optical section, appearing in the mucosa with chronic atrophy gastritis. **B**, The conventional histologic features of type E. The number of pits decreasing and the lumens of pits prominently dilating can be seen, and the atrophy is apparent (H&E, orig. mag. $\times 200$).

of inflammation were as follows. Inflammation in the type A group was mild in 17.4%, moderate in 5.5%, and absent in the others. In the type B group, it was mild in 11.8%, moderate in 23.7%, and severe in 58.1%. Compared with the type A group, the inflammatory degree in the type B group was significantly higher ($P < .001$). Among the 38 sites classified as type C and 180 sites classified as type D, the histopathologic results on grading of inflammation were as follows. Inflammation in the type C group was mild in 15.8%, moderate in 7.9%, and absent in the others. In the type D group, it was mild in 13.3%, moderate in 18.3%, and severe in 56.7%. The inflammatory degree in

Figure 7. The confocal image of type F and the histopathologic features of type F. **A**, Villus-like appearance, interstitium in the center (*blue arrow*), and black goblet cells (*white arrows*) appearing, indicating intestinal metaplastic mucosa. The epithelial cells (*red arrow*) are more slender and brighter than normal gastric epithelial cells. **B**, The conventional histopathologic features of type F. Marked intestinal metaplasia can be seen (H&E, orig. mag. $\times 200$).

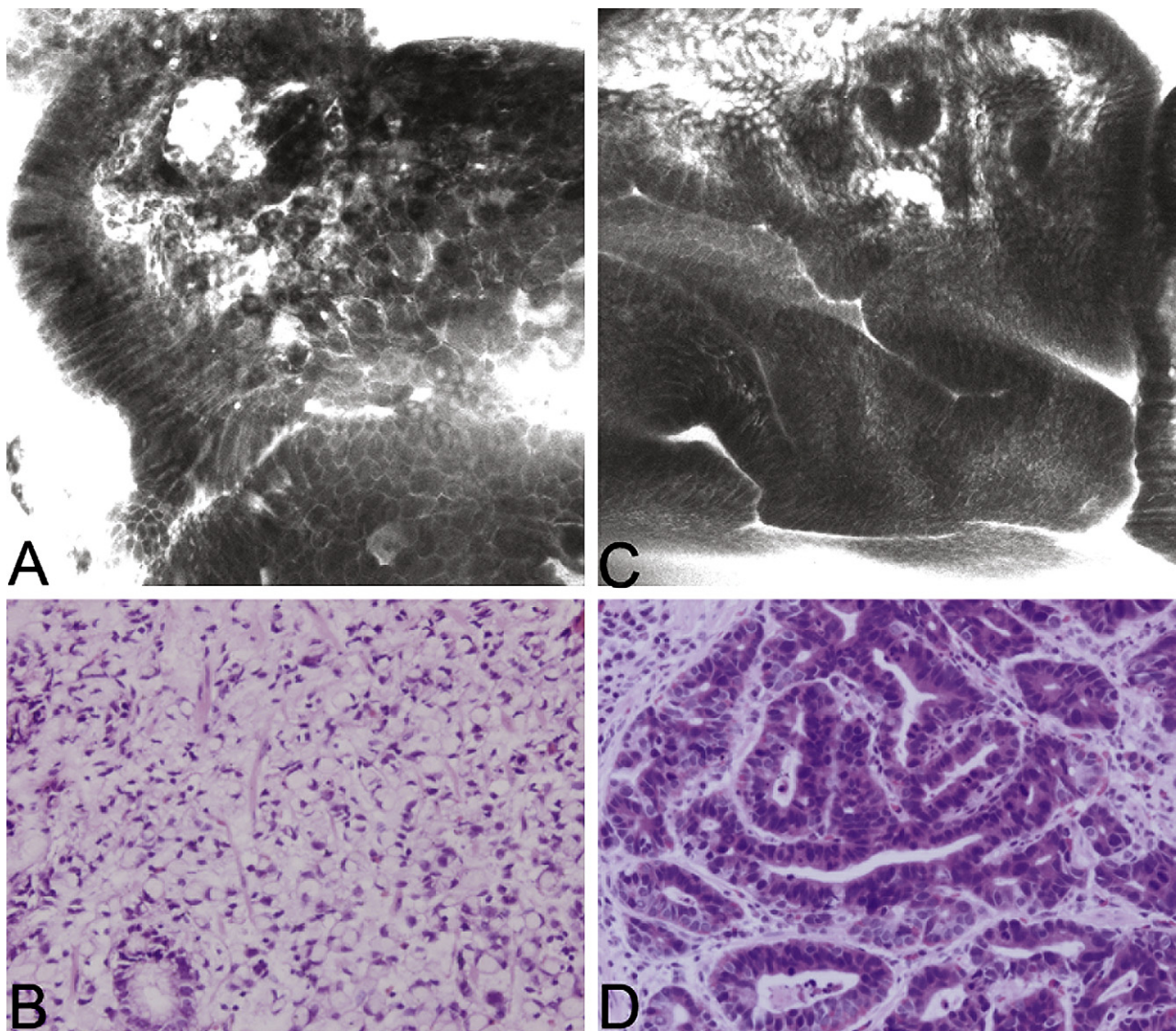


Figure 8. The confocal image and the histopathologic features of type G. **A**, The pattern of type G₁, normal pits disappearing, with the appearance of diffusely atypical cells. **B**, The cross-sectional histopathologic finding is signet-ring cell carcinoma (H&E, orig. mag. ×400). **C**, The pattern of type G₂, normal pits disappearing, with the appearance of atypical glands. **D**, The cross-sectional histopathologic finding is differentiated tubular adenocarcinoma (H&E, orig. mag. ×400).

the type D group was significantly higher than that in the type C group ($P < .001$). Table 1 shows the sensitivity, specificity, accuracy, PPV, and NPV of the type E pattern for predicting gastric atrophy, the type B' + D' pattern for moderate to severe neutrophil activity and the type G pattern for gastric cancer. In gastric intestinal metaplastic mucosa, the goblet cells showed large black cells because mucin in goblet cells was not stained by fluorescein sodium, and they were easily distinguished.

DISCUSSION

The change and abnormality of the gastric pit pattern is the basis of diagnosis made by magnifying gastroendoscopy. Although confocal endomicroscopy produces high-

magnification images of surface and subsurface tissues of the GI tract at the cellular level, the images obtained by confocal endomicroscopy are cross-sectional. So the change in the pattern of gastric pits, which are the basic structural unit of the gastric mucosa, is also very important for the confocal endomicroscopic diagnosis.

There have been several reports on the potential use of magnifying endoscopy for the diagnosis of histologic gastritis. The studies demonstrated that the patterns of magnifying endoscopic appearance, including gastric pit pattern, were specific enough for the diagnosis of histologic gastritis and that mucosal inflammation was reflected on the surface structure. Moreover, active inflammation and intestinal metaplasia could be distinguished by magnifying endoscopy on the basis of the surface structure.³⁻⁶

TABLE 1. The sensitivities, specificities, accuracy, PPVs, and NPVs of various confocal findings for the prediction of atrophy, moderate to severe activity, and gastric cancer

Histologic lesion	Pit pattern	Sensitivity (% [95% CI])	Specificity (% [95% CI])	Accuracy (% [95% CI])	PPV (% [95% CI])	NPV (% [95% CI])
Atrophy	Type E	83.6, 56/67 (74.7-92.5)	99.6, 452/454 (98.4-100.0)	97.5, 508/521 (96.2-98.8)	96.6, 56/58 (87.6-99.7)	97.6, 452/463 (96.2-99.0)
Moderate to severe activity	Type B' + D'	81.9, 86/105 (74.5-89.3)	99.3, 413/416 (97.9-99.9)	95.8, 499/521 (94.1-97.5)	96.6, 86/89 (99.3-90.1)	95.6, 413/432 (93.7-97.5)
Gastric cancer	Type G	90.0, 18/20 (68.0-99.0)	99.4, 488/491 (98.2-99.9)	97.1, 506/521 (95.7,98.6)	85.7, 18/21 (64.0-97.0)	97.6, 488/500 (96.3-98.9)

Confocal endomicroscopy generates 1000× magnification virtual histologic images of tissue; therefore, it can provide more information on gastric pits, epithelial cells, interstitium, and the lumens of pits. In addition, the confocal images are images of consecutive optical sections, so not only the surface but also the subsurface structures of gastric pits can be observed. As a result, the prediction of the histopathologic diagnosis by using confocal endomicroscopy has been improved. The mucous layer can not be completely scanned by confocal endomicroscopy because the depth of scanning is only 250 μm, so in the current study to identify the accuracy of the classification of gastric pit patterns in gastritis, the pit patterns were compared with the conventional histopathologic findings instead of cross-sectional histopathologic findings. The current study demonstrated that confocal endomicroscopy was able to visualize precisely the structure of the pit, and the pit pattern of normal mucosa was obviously different from that of histologic gastritis. The pit patterns of normal mucosa with fundic and pyloric glands were mainly types A and C, respectively, and with chronic gastritis the pit patterns showed the change of type A to type B and type C to type D. The current study also demonstrated that the inflammatory degree in mucosa with type B was significantly higher than that in type A, whereas that in type D was significantly higher than that in type C. With inflammatory infiltration extending deeper into the mucosa and progressive distortion and destruction of the glands, atrophic gastritis appeared, and the confocal endoscopic pit pattern became type E. Type E was specific enough for the histologic diagnosis of atrophy. Because goblet cells were easily distinguished by confocal endomicroscopy, it was a very sensitive method for the diagnosis of intestinal metaplasia.

On the other hand, because confocal images are obtained in vivo, morphologic, functional, and pathologic factors in tissue will influence the fluorescent staining patterns observed,¹⁷ which can reflect the pathophysiologic process to some extent. In the current study, our preliminary findings showed that the widened and brightened interstitium could be seen in some of the confocal images obtained from the sites of active inflammation. It might be due to the strengthening of fluorescent staining in the

interstitium caused by the increase in hyperemia and effusion in the active inflammatory region. In addition, the destruction of epithelial cells resulting from active inflammation showed the defect of topical epithelial cells in the confocal images. Our study demonstrated that the 2 images above were specific for diagnosing moderate to severe neutrophil activity.

Many gastric diseases, including gastric cancer, are often associated with *Helicobacter pylori*-positive gastritis, so it is clinically necessary to diagnose and grade gastritis. Performing multiple biopsies has been the only way to assess the grade of gastritis to date, but biopsy is invasive, which may cause bleeding in patients receiving anticoagulant therapy. Our findings suggest the diagnostic potential of confocal endomicroscopy for assessing histologic gastritis.

Moreover, confocal endomicroscopy has specific advantages in diagnosing early gastric cancer. The character of real-time virtual histologic imaging in vivo is considered as "optical biopsy." Compared with biopsy, its advantages are no bleeding and it can be done at more sites. Today, although conventional histology is still a gold standard of diagnosis, endoscopists can take advantage of confocal endomicroscopy to select appropriate biopsy sites in suspicious lesions, which enhances the positive rate of biopsy as much as possible.

Through the method of immunohistochemistry, as documented by Odagi et al,¹⁸ fluorescein-positive staining was seen in the interstitium, capillary walls, the cytoplasm of mucosal surface enterocytes, and the mucosal surface of crypts after intravenous administration of fluorescein sodium. Because fluorescein sodium is not enriched in the nuclei of epithelial cells after systemic administration because of its pharmacokinetic properties, the nuclei are not readily visible in the confocal images when this agent is used.¹ However, the resolution of confocal images is remarkably high (lateral resolution of 0.7 μm), therefore, epithelial cells, vasculature, and interstitium can be clearly distinguished. So the characteristic atypical architecture of malignant tumor is easily identified. In the current study, atypical glands and cancer cells were easily distinguished; as a result, the correct diagnosis could be reached on the

basis of a simple standard, although the nuclei could not be visualized in confocal images.

Although the study was designed as accurately and completely as possible, the exploratory nature of the study made it difficult to avoid all limitations. To improve the accuracy of the classification, the confocal images were evaluated by 2 investigators (in consensus). In addition, the endoscopists who participated in the study were not sufficient in number to avoid the bias from sampling in readers. Therefore, inter-observer and intraobserver variability was not evaluated. An independent observer agreement study should be conducted in a separate study that is specifically designed for the purpose, and training of readers and selecting readers according to random sampling are necessary.

In conclusion, at present, confocal endomicroscopy cannot completely replace conventional histopathologic examination, but confocal endomicroscopy can evidently improve the prediction of the histopathologic diagnosis. However, the classification system should be tested with a larger sample.

DISCLOSURE

The authors report that there are no disclosures relevant to this publication. The confocal endomicroscope was provided by Pentax, Tokyo, Japan. No additional grant or financial incentive was provided from manufacturers mentioned in this study. This study was funded by Shandong Province Science and Technology Committee (2006GG3202022).

REFERENCES

1. Kiesslich R, Goetz M, Vieth M, et al. Confocal laser endomicroscopy. *Gastrointest Endoscopy Clin North Am* 2005;15:715-31.
2. Evans JA, Nishioka NS. Endoscopic confocal microscopy. *Curr Opin Gastroenterol* 2005;21:578-84.
3. Kim S, Haruma K, Ito M, et al. Magnifying gastroendoscopy for diagnosis of histologic gastritis in the gastric antrum. *Dig Liver Dis* 2004;36:286-91.
4. Yagi K, Honda H, Yang JM, et al. Magnifying endoscopy in gastritis of the corpus. *Endoscopy* 2005;37:660-6.

5. Dinis-Ribeiro M, da Costa-Pereira A, Lopes C, et al. Magnification chromoendoscopy for the diagnosis of gastric intestinal metaplasia and dysplasia. *Gastrointest Endosc* 2003;57:498-504.
6. Kim S, Ito M, Haruma K, et al. Surface structure of antral gastric mucosa represents the status of histologic gastritis: fundamental evidence for the evaluation of antral gastritis by magnifying endoscopy. *J Gastroenterol Hepatol* 2006;21:837-41.
7. Yang JM, Chen L, Fan YL, et al. Endoscopic patterns of gastric mucosa and its clinicopathological significance. *World J Gastroenterol* 2003;9:2552-6.
8. Tajiri H, Doi T, Endo H, et al. Routine endoscopy using a magnifying endoscope for gastric cancer diagnosis. *Endoscopy* 2002;34:772-5.
9. Tanaka K, Toyoda H, Kadowaki S, et al. Features of gastric cancer and gastric adenoma by enhanced-magnification endoscopy. *J Gastroenterol* 2006;41:332-8.
10. Yoshida T, Kawachi H, Sasajima K, et al. The clinical meaning of a non-structural pattern in early gastric cancer on magnifying endoscopy. *Gastrointest Endosc* 2005;62:48-54.
11. Kiesslich R, Bure J, Vieth M, et al. Confocal laser endoscopy for diagnosing intraepithelial neoplasias and colorectal cancer in vivo. *Gastroenterology* 2004;127:706-13.
12. Kiesslich R, Hoffman A, Goetz M, et al. In vivo diagnosis of collagenous colitis by confocal endomicroscopy. *Gut* 2006;55:591-2.
13. Kakeji Y, Yamaguchi S, Yoshida D, et al. Development and assessment of morphologic criteria for diagnosing gastric cancer using confocal endomicroscopy: an ex vivo and in vivo study. *Endoscopy* 2006;38:886-90.
14. Kitabatake S, Niwa Y, Miyahara T, et al. Confocal endomicroscopy for the diagnosis of gastric cancer in vivo. *Endoscopy* 2006;38:1110-4.
15. Dixon MF, Genta RM, Yardley JH, et al. Classification and grading of gastritis, the updated Sydney System: International workshop on the histopathology of gastritis, Houston 1994. *Am J Surg Pathol* 1996;20:1161-81.
16. Hamilton SR, Aaltonen LA, editors. World Health Organization classification of tumors: pathology and genetics of tumors of the digestive system. Lyon: IARC Press; 2000. p. 38-52.
17. Polglase AL, McLaren WJ, Skinner SA, et al. A fluorescence confocal endomicroscope for in vivo microscopy of the upper and the lower GI tract. *Gastrointest Endosc* 2005;62:686-95.
18. Odagi I, Kato T, Tajiri H. A study of normal intestine using confocal endomicroscopy [abstract]. *Gastrointest Endosc* 2006;63:AB220.

Received April 9, 2007. Accepted January 31, 2008.

Current affiliations: Department of Gastroenterology (J.-N.Z., Y.-Q.L., Y.-A.Z., T.Y., Y.-T.G., H.L.), Department of Pathology (J.-P.Z.), Qilu Hospital, Shandong University, Jinan, Shandong Province, China.

Reprint requests: Yan-Qing Li, MD, PhD, Department of Gastroenterology, Qilu Hospital, Shandong University, No. 107, Wenhua Road, Jinan, PR China.

Moving

To ensure continued service please notify us of a change of address at least 6 weeks before your move.

Phone Subscription Services at 800-654-2452 (outside the U.S. call 407-345-4000), fax your information to 407-363-9661, or e-mail elspcs@elsevier.com.